ARTICLE

Multiple Plasmonic Resonances and Cascade Effect in Asymmetrical Ag Nanowire Homotrimer

Yue Li, GuangTao Fei*, Shao-hui Xu, Guo-liang Shang, Hao-miao Ouyang, Li-de Zhang

Key Laboratory of Materials Physics, and Anhui Key Laboratory of Nanomaterials and Nanotechnology, Institute of Solid State Physics, Hefei Institutes of Physical Science, Chinese Academy of Sciences, Hefei 230031, China.

(Dated: Received on February 26, 2016; Accepted on March 22, 2016)

Plasmonic Ag nanowire homotrimer with asymmetrical radii and separations, which exhibits characteristics of multiple plamonic resonances and different electric field distributions, is systematically investigated by means of 2D finite element method. It was found that the dark and bright modes appear in asymmetrical nanowire homotrimer. In addition, when the dark modes appear between the smaller radii of the nanowires, the cascade effect results in enhanced electric field between the smaller radii nanowires. As a result of the appearance of the bright modes between the smaller radii of the nanowires, the restriction of the cascade effect generates enhanced electric field between the bigger nanowires.

Key words: Asymmetric homotrimer, Bright and dark modes, Extinction cross section, Cascade effect

I. INTRODUCTION

Induced by an incident electromagnetic field of a given frequency, metal nanostructures can sustain localized surface plasmon (SP) resonances, arising from the coherent collective oscillation of conduction electrons in metal surfaces [1−5]. Generally, only a single resonance peak exists in the individual nanostructure, which is considered as its natural plasmonic dipole mode, while multiple plasmonic resonances can be observed in nano-complex. For the symmetrical nano-complex, it has been reported that the resulting electromagnetic field displays symmetrical distribution in the approaching area mainly through plasmon coupling [6−8]. However, due to the symmetrically distribution, the symmetrical nano-complex can only present homogeneous but limit plasmon modes. As a result, the symmetrical nano-complex has less extraordinary properties, which limits its wide application in many areas, such as sensing, medicine, catalysis, and optoelectronics.

Recently, different asymmetric nano-complexes have been theoretically and experimentally studied [9−11]. The absence of symmetry has demonstrated that the spectrum is not solely a linear combination of the plasmonic modes of the individual nanostructures, which is highly beneficial for manipulating the line shapes of the spectrum and the electromagnetic phenomena between the individual nanostructures. As a prototype, in the asymmetric Ag homotrimer with decreasing sizes and separations, it is found that the resulting electric field enhancement is enhanced by orders of magnitude in the gap between the smallest nanospheres, this phenomenon is referred as the cascade effect [4]. However, the mechanism of the appearance of the different electric field associated with the plasmonic modes in asymmetric nanosphere homotrimer is not clearly interpreted.

Metal nanowires with cross sections below the free-space diffraction limit of light support the propagation of surface plasmons that confines light into nano-scale dimensions. Furthermore, compared to the assembly of the nano-complexes with complex nanofabrication process, metal nanowires are relatively easy to prepare in a repeatable and reliable manner, making these nanostructures widely used in sub-wavelength optics, nanoscale optical components and devices [12, 13]. Most studies have been reported on the surface enhanced Raman scattering, propagation, scattering properties of metal nanowires with symmetrical parameters [14−16].

In this work, we systematically investigate the plasmonic properties of the homotrimers based on the asymmetrical metal nanowires. We find that the asymmetrical homotrimer can present bright or dark modes at the resonance wavelengths. Especially for the homotrimer case, the cascade effect can result in different electric field distributions in the approaching area of the nanowires, depending on the dark or the bright modes appearing between the smaller radii of the nanowires. When the dark mode appears between the smaller nanowires, the corresponding area shows higher electric field than that between the bigger nanowires, which is referred as the cascade effect. In contrast, the

*Author to whom correspondence should be addressed. E-mail: gtfei@issp.ac.cn, Tel.: +86-551-65591453, FAX: +86-551-65591434

existence of the bright mode between the bigger nanowires will result in the restriction of the cascade effect, leading to the higher electric field. Our investigation shows different results from the symmetric case, essentially arising from the appearance of the bright and dark modes while the nanowire homotrimers is symmetry breaking.

II. MODEL AND NUMERICAL METHOD

In present work, the optical properties of size-asymmetrical Ag homotrimer nanowires are calculated using 2D finite element method model based on Maxwell's equations, which has been comprehensively described in Ref.[17]. Meanwhile, the proposed perfectly matched layer are placed before the outer boundary to avoid nonphysical reflections of outgoing electromagnetic waves. Throughout this work, the metal in our model is Ag. The permittivity data of Ag are obtained from Johnson and Christy [18]. And the whole calculations performed for homotrimer nanowires are immersed in a surrounding medium of air.

III. RESULTS AND DISCUSSION

We adopt model morphology of Ag homotrimer nanowires (Fig.1) with different radii and separations to investigate their optical properties, where R_1, R_1, and R_3 are the radii, S_1 and S_2 are the surface-to-surface separations between the 1st and 2nd, the 2nd and 3rd nanowires, respectively. In all the calculations presented here, the direction of the incident wave-vector K is along the y-axis and electric-field polarization vector is parallel to the x-axis (see Fig.1). Besides, the infinitely long wires orients along the z direction.

Empirically, the plasmonic resonances of homotrimer can be investigated by dividing into two homodimer. Hence we start our investigation on the optical properties of two plasmonic homodimers with radii R_1 and R_2, R_2 and R_3, respectively. In addition, for the model with asymmetrical parameters, the calculated curves of extinction cross section (ECS) are not smooth with insignificant kinks as that in the symmetric case. Therefore, the following discussions would focus on the significant resonance peaks to study the multiple coupling, the negligible differences of ECS are outside the discussion range of our interest.

A. Two asymmetrical homodimers with respective radii R_1 and R_2, R_2 and R_3

The two homodimers with radii R_1=100 nm and R_2=50 nm, R_1=50 nm and R_2=25 nm are referred to homodimer-1 (H1) and homodimer-2 (H2), respectively. The ECS spectra of H1 and H2 with separation S=2 nm

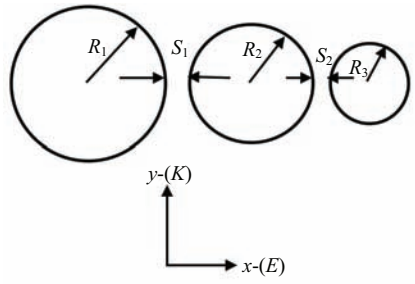

FIG. 1 Schematic model morphology of the studied asymmetrical Ag nanowire homotrimer with the configurable parameters and the incident polarization parallel to the dimer axis.

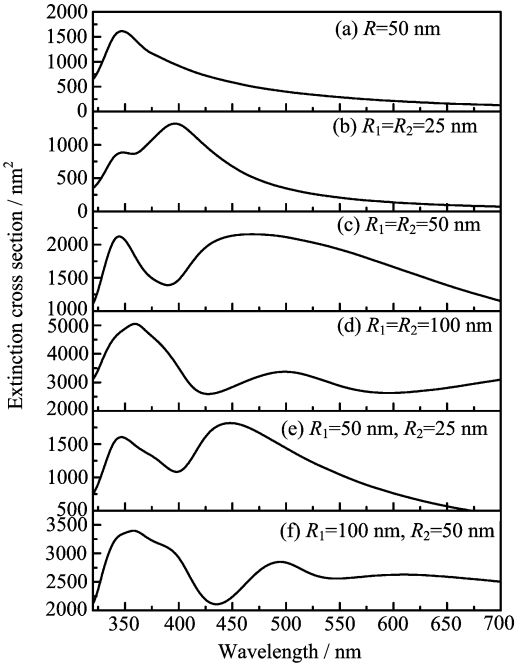

FIG. 2 The extinction cross sections of (a) single nanowire, (b)−(d) symmetrical homodimer nanowire with separation S=2 nm, (e) and (f) asymmetrically nanowire with separation S=2 nm.

are simulated. For comparison, the ECS of the individual and symmetrical homodimer nanowire is also shown in Fig.2. While an individual nanowire with equal radii to that in our model, namely, 25, 50, and 100 nm, respectively, it only has one resonance peak arising from a dipole around 342 nm (Fig.2(a)). When the individual nanowire forms the symmetrical homodimer structures (Fig.2 (b)−(d)), there exist multiple resonance peaks, which correspond to the dipolar and multiple higher-order modes, arising from the phase retardation effects [19, 20]. In plasmonics, the corresponding charge distributions can be used to clearly verify the involved plasmon modes at resonance wavelengths [1, 20], therefore the charge distribution of the homodimer with radii R_1=R_2=100 nm along x direction at three resonance

DOI:10.1063/1674-0068/29/cjcp1602030

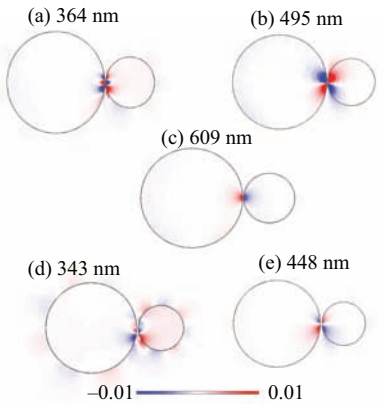

FIG. 3 The corresponding charge distribution along the x direction at the resonance wavelengths for (a)−(c): H1, (d) and (e): H2 with the separation S=2 nm. The color bar shows the varied values of the charge density distribution.

wavelengths is calculated (Fig.S1 in supplementary materials). It can be found that the higher-order modes of the triakontadipolar and quadrupolar (Q) mode correspond to the resonance wavelengths of 359 and 497 nm, respectively, and the dipolar (D) mode corresponds to the resonance wavelengths of 826 nm, which is out of visible light.

For the asymmetrical case of H2 and H1 in Fig.2 (e) and (f), compared with the symmetrical homodimer case, there also exist the multiple resonance peaks, located at 364, 495, and 609 nm for H1, 343 and 448 nm for H2, respectively. The charge distributions at resonance peaks of the two asymmetrical homodimers for S=2 nm are shown in Fig.3. For H1 at wavelengths of 364, 495, and 609 nm, six, four, and two nodes can be clearly observed in the approaching area, as expected, which is corresponding to higher-order octupolar (O), Q and D modes, respectively (Fig.3(a)−(c)). For H2, surprisingly, both higher-order Q modes appear at the wavelengths of 343 and 448 nm, respectively (Fig.3 (d) and (e)). These results are different from that of the symmetrical case, especially for the H2. That is, the symmetrical homodimer (Fig.2 (b) and (c)) with two resonance peaks shows the O and D modes at 340 and 499 nm (not shown in this work).

The ECS spectra of the two homodimers with varied separations and radii are shown in Fig.S2 (supplementary materials). The corresponding charge distributions at the resonances of H1 and H2 with S=4 nm are highlighted in Fig.S3 (supplementary materials). One can note that, when S increases to 4 nm, the charges are less than that of the corresponding S=2 nm (Fig.3), therefore resulting in weakened SP coupling. When S finally increases to 20 nm, there only exists a resonance peak (Fig.S2 (a) and (b) in supplementary materials) arising from the weakened SP coupling, which is analogous to the dipole resonance peak of the single nanowire around 342 nm. Different from the results by increasing the separation, the increasing radius of the homodimer generates much higher-order modes with asymmetrical line shapes (Fig.S2(c) in supplementary materials), arising from the phase retardation effects, which is analogous to the asymmetrical Au:Ag heterodimers on increasing the size of dimer size [21].

In the plasmonic nanostructures with symmetry breaking, the bright mode and dark mode are involved. Naturally, the bright mode possesses finite dipole moment, which can be excited by the incident light efficiently. In contrast, the dark plasmon mode with near-zero dipole moment, couples to light less effectively [22]. However, the dark mode can be excited by the electric field associated with the bright mode [22, 23]. In addition, the exclusive losses of dark mode are only limited by the intrinsic metal losses, which is much lower than the radiative damping of the bright mode. Therefore, the dark mode will result in enhanced and localized electric field distribution than that of the bright mode [24, 25]. In our models, for the morphology of H1 with asymmetrical radii, it can be clearly observed from the ECS (Fig.2 (e) and (f)) that the D at 609 nm is much broader than the O and Q at 364 and 495 nm. Combinly this feature with the charge distributions (Fig.3 (a)−(c)), we can conclude that the D mode is referred to the superradiant bright mode, and higher-order (O and Q) modes are referred to the subradiant dark mode, respectively. For H2, there is only dark Q mode. However, different from the classic nanostructure with the dark modes directly excited by the bright modes such as the disk-ring plasmonic nanostructures [1, 9], the appearance of the so-called dark modes in nanowire arrays arises from the splitting of the dipole modes in the individual nanowire to reduce the Coulomb repulsion energy [26, 27]. This feature can be confirmed in Fig.S2 (a) and (b) (supplementary materials). As the separation increases from 2 nm to 20 nm, owing to reduced mode repulsion, the ECS spectrum of homodimer is comparable with the individual nanowire with a dipole mode.

Based on the above results, the plasmonic properties of the asymmetrical nanowire homotrimer consisting of H1 and H2 are investigated. The different plasmon modes can be excited in H1 and H2. In addition, the bright and dark modes generate distinguished electric field distribution in the approaching areas of the homotrimer consisting of the H1 and H2.

B. Asymmetrical homotrimer with varied separation and radius

As expected, electromagnetic coupling can be modulated by changing the separation and radii of the homotrimer consisting of the H1 and H2 as investigated above. Here we adopt the configurations with the varied radii and separations simultaneously.

DOI:10.1063/1674-0068/29/cjcp1602030

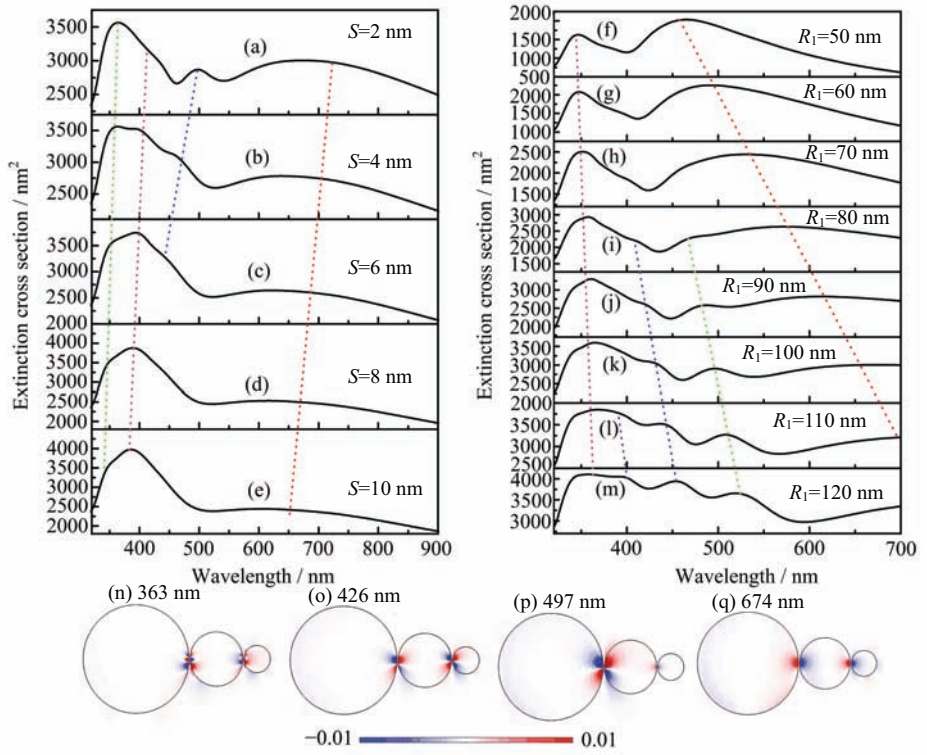

FIG. 4 The dependence of the ECS spectra of asymmetrical Ag nanowire homotrimer on the varied separations S=S_1=S_2 with constant R_1:R_2:R_3=100 nm:50 nm:25 nm (a−e) and the radii of the asymmetrical homotrimer with the same scale R_1:R_2:R_3=4:2:1, separations S_1=S_2=2 nm (f−m). The charge contribution of the resonance peaks along the x direction for the separations 2 nm with R_1:R_2:R_3=100 nm:50 nm:25 nm of homotrimer (n) 363 nm, (o) 497 nm, (p) 497 nm, and (q) 674 nm. The dashed lines with different colors present the variation of the multiple resonance peaks. The color bar shows the varied values of the charge density distribution.

1. Varied separations S_1=S_2 with R_1:R_2:R_3=4:2:1 nm

The dependence of the ECS spectra of asymmetrical Ag nanowire homotrimer with uniform R_1:R_2:R_3=100 nm:50 nm:25 nm on the varied separations S_1=S_2=S is shown in Fig.4 (a)−(e), and dependence of the ECS spectra of the homotrimers with R_1:R_2:R_3=4:2:1 and S_1=S_2=2 nm on the varied radius is shown in Fig.4 (f)−(m). We can note that when S decreases or the radius increases, the multiple resonance peaks can be gradually and clearly observed. For the reference state, we would firstly focus our attention on the homotrimer configuration with S_1=S_2=2 nm and uniform R_1:R_2:R_3=100 nm:50 nm:25 nm (Fig.4(a)) to get insight into the tunability of electromagnetic coupling and multiple resonances. The corresponding charge distribution at the four obvious resonance peaks located at 674, 497, 426, and 363 nm are plotted in Fig.4 (n)−(q), respectively, and the corresponding values of electric field along the x direction are listed in Table I. Here, most part of the electric filed (not shown here) and charge distribution locate around the approaching area. It is worth mentioning that the resulting resonance peaks at 363, 426, and 497 nm with asymmetrical line shapes are comparable with the Fano resonances originated from the coupling of the super-radiant modes and subradiant modes, which have been found in nanocomplexes with symmetry breaking [9].

TABLE I The corresponding near field of the resonance peaks along the x direction for the separations 2, 4, and 6 nm, E_1 is the maximum values between the bigger nanowires, E_2 is for the smaller nanowires.

Separation/nm	Wavelength/nm	E_1/(V/m)	E_2/(V/m)
2	674	19	11
	497	33	7
	426	12	36
	363	8	15
4	634	13	9
	450	16	7
	403	8	19
	362	7	11
6	623	9	6
	441	10	4
	396	7	12
	360	7	11

From the charge distributions in Fig.4 (n) and (p)

DOI:10.1063/1674-0068/29/cjcp1602030

for S=2 nm, it can be found clearly that there exist all dark O modes between two homodimers with six charge nodes at 363 nm of the resonance wavelength, all Q modes with four charge nodes at 426 nm of the resonance wavelength, the bright D (50 nm:25 nm homodimer) and dark Q (100 nm:25 nm homodimer) modes with two and four charge nodes in the case of the third resonance at 497 nm, respectively. Different from the appearance of the higher-order modes, the resonance at 674 nm (Fig.4(p)) corresponds to the dipolar bright mode, leading to a spectral broadening because of the radiative damping [1, 2].

In virtue of the existence of the bright and dark modes distributed in the gaps for the model with S=2 nm and varied radii shown in Fig.4 (f)−(m), not only the appearance of different plasmon modes, but also the near field distribution of the size-asymmetrical nanowires is greatly influenced. Previous works has been reported that a self-similar linear chain, consisting of three Ag nanospheres with decreasing sizes and separations, can produce local field enhancement in the gaps between the smaller particles due to so-called cascade effect [4]. That is, while the external field impinges on the cascaded nanospheres, the local optical field between the large particles is enhanced firstly, and then the enhanced electric field acts on the smaller particles as an excitation field, resulting in higher nanofocusing than that in bigger ones.

In our model, due to the multiple resonance peaks with complex mode distribution, the near field distributions of size-asymmetrical homotrimer nanowires with four resonance peaks (listed in Table I for symmetrical separations 2 nm) present different results. For the wavelengths of 674 and 497 nm, the maximum electric field localizes at the gap between the two larger nanowires (E_1). In contrast, the maximum electric field localizes at the gap between the two smaller nanowires (E_2) for the wavelengths of 426 and 363 nm. These phenomena can be explained as the association of the cascade effect with the different plasmon mode appearing between the smaller radii of the nanowires. Due to the fact that the losses of dark mode with the intrinsic metal losses are much lower than the radiative damping of the bright mode [24, 25]. When the dark mode, which can be able to store a larger amount of electromagnetic energy than the bright mode, appears between the two smaller nanowires, the cascade effect will results in bigger electric field distributed between the two smaller nanowires. In constrast, the appearance of the bright mode, which has radiative damping, will lead to the restriction of the cascade effect, hence the resulting bigger electric field distributed between the two bigger nanowires.

Based on the above interpretation of the multiple resonances and the different electric field distribution in the separations of S_1=S_2=2 nm model, now we turn our attention to analyze the plasmon resonance as a function of separations S as shown in Fig.4 (b)−(e). One can note that with increasing of separations, the resonance peaks are all blue-shift. This phenomenon can be interpreted that as the separation increases, the resulting splitting of the plasmon modes to reduce the Coulomb repulsion energy between the individual nanowire decreases [26, 28, 29]. For the case of separations of S_1=S_2=4 nm (Fig.4(b)), there also exist four apparent resonance peaks at 362, 403, 450, and 634 nm as that for S=2 nm. As S increases, the first resonance (corresponding to 362 nm for the separations of S_1=S_2=4 nm) keeps almost constant for the S_1=S_2>4 nm. The charge distribution of the resonance peaks for S_1=S_2=4 nm are represented in Fig.S4 (supplementary materials), presenting that the resonance at 362 nm exhibits the mixture of the dark Q and O modes (Fig.S4(a) in supplementary materials), compared to the pure O modes in homotrimer with S_1=S_2=2 nm at 363 nm (Fig.4(n)). The resonance at 403 nm for the homotrimer with the separations of S_1=S_2=4 nm is all dark Q modes (Fig.S4(b) in supplementary materials). The mode distributions of the resonance at 450 nm (Fig.S4(c) in supplementary materials) are comparable with S_1=S_2=2 nm at 497 nm (Fig.4(p)), resulting in the same electric field distribution between the bigger nanowires, arising from the ineffectively cascade effect. However, for the separations of 4 nm at 362 and 403 nm, due to the disappearance of superradiant bright mode, the SP interaction between the bigger homodimer nanowires generates an excitation field, and then the enhanced near field (E_2) (observed in Table I) stays in the gap of the smaller as a result of the cascade effect [4]. Furthermore, for the separation of 4 nm, the SP interaction between the nanowires decrease compared with that of the separation of 2 nm, this brings about the decreasing near field of the whole system, especially for E_1 listed in Table I. Above all, we can conclude that the cascade effect takes effect to confine the near field in the gap of the smaller nanowires, while the pure dark modes exist at the corresponding resonance wavelength.

In Fig.4 (f)−(m), one can note that when the radius of the homotrimer increases, together with the same scale R_1:R_2:R_3=4:2:1 and separations S_1=S_2=2 nm, more resonance peaks and asymmetrical line shapes can be observed, indicating that the higher order resonance modes are excited [19, 20]. The resonance peak at 343 nm for R_1=50 nm homotrimer, which corresponds to dipolar mode. These results are comparable with the size-dependent of the homodimer as shown in Fig.2 (f)−(m). In summary, we can conclude that, due to the decrement of the separation or the increment of the radii, the resulting increment of the SP coupling between the asymmetrical nanowires generates multiple resonance peaks. At respective resonance peak wavelength, the bright and dark modes modulate the role of the cascade effect, and producs different electric field distributions.

DOI:10.1063/1674-0068/29/cjcp1602030

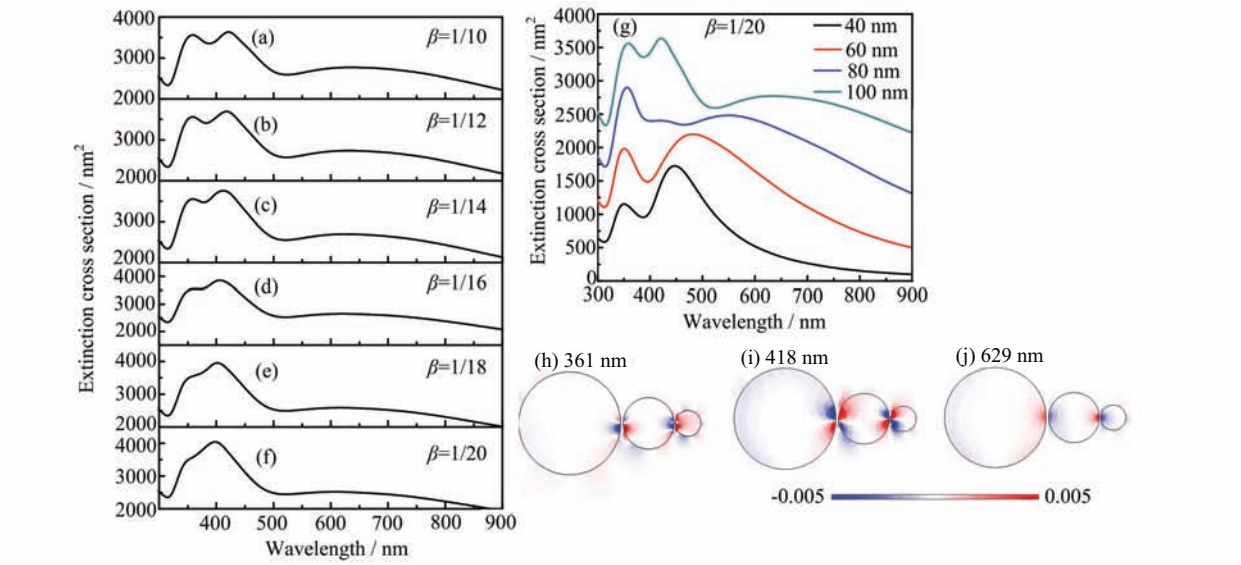

FIG. 5 The extinction spectra of asymmetrical Ag homotrimer nanowires with R_1=100 nm, R_2=50 nm, and R_3=25 nm for (a)−(f) different ratios β, (g) β =1/20 (S_1=5 nm and S_2=2.5 nm) for varied radii. (h)−(j) show the charge contribution of the resonance peaks for the ratio β=1/20 in (f). The color bar shows the varied values of the charge density distribution.

2. Varied ratios of separations S_1=2S_2 with R_1:R_2:R_3=4:2:1

The influence of asymmetrical separations and radii on the optical properties of homotrimer nanowires as Li's assumption is investigated [4]. We set the quantitative relation of radii and separations as R_{i+1}=αR_i, $S_{i+1,i+2}$=$\alpha S_{i,i+1}$, and $S_{i,i+1}$=βR_i, where α=1/2 in current model is constant as the reference state. The ECS spectra of asymmetrical Ag nanowire homotrimer with R_1=100, R_2=50, and R_3=25 nm for different ratios β is shown in Fig.5(a)-(f), β=1/20 (S_1=5 nm, S_2=2.5 nm) for different radii is shown in Fig.5(g), and the corresponding charge distributions at the resonance peaks in Fig.5(f) are highlighted in Fig.5 (h)−(j). Meanwhile, the values of the near field at the resonance peaks for β=1/20 and 1/18 are also listed in Table II. For ECS spectrum of the ratio 1/20 in Fig.5(f), one can note that there exist three resonance peaks at 629, 418, and 361 nm, respectively. The bright dipolar mode at 629 nm confirmed by the charge contribution in Fig.5(j) is also broadened due to its radiative damping. However, for the resonance at 418 nm, dark Q modes appeared in the gap of the nanowires (Fig.5(i)), when Q and hexapolar modes for the resonance are at 361 nm (Fig.5(h)), which are the same as the modes as stated above with the separations S_1=S_2=4 nm. In addition, the higher near-fields at 418 and 361 nm are distributed significantly in the gap of the smaller homodimer (Table II), indicating that the cascade effect functions effectively in virtue of the asymmetrical sizes and separations due to the absence of the dipolar mode (Fig.5 (h) and (i)). However, the cascade effect is less effective at 629 nm because of the damping of dipolar modes as presented in the above discussion.

TABLE II The corresponding near field of the resonance peaks for the ratios 1/20 and 1/18, E_1 is the maximum values between the bigger nanowires, E_2 for the smaller nanowires.

β	Wavelength/nm	E_1/(V/m)	E_2/(V/m)
1/20	629	11	10
	418	13	27
	361	7	12
1/18	624	9	11
	415	8	25
	362	5	10

As shown in Fig.5(a), it is noted here that, as the separation (the ratio β) increases to S_1=10 nm and S_2=5 nm (β=1/10), the resonance at 418 nm for β=1/20 has blue-shift to 415 nm slightly, and the resonance at 361 nm almost keep unchanged, retaining a significant peak at 389 nm, arising from the weakened SP coupling. It indicates that the symmetry-breaking of the sizes and separations of Ag nanowire homotrimer generates more effective cascade effect.

So far, we have performed the calculations using large nanowires with asymmetrical separations. Next, the homotrimers with simultaneously varied radii and separations are investigated. The optical ECS spectra as a function of the sizes with constant ratio β=1/20, α=1/2 are shown in Fig.5(g), and the corresponding near field of the resonance peaks are listed in Table III. When the sizes and the separations of the nanowires get smaller, the spectrum of the dipolar bright mode becomes narrower, arising from the decreasing radiative damping. Furthermore, due to the cascade effect, the near fields

DOI:10.1063/1674-0068/29/cjcp1602030

TABLE III The corresponding near field of the resonance peaks for the varied size with constant ratios 1/20, E_1/(V/m) is the maximum values between the bigger nanowires, E_2/(V/m) for the smaller nanowires.

R_1:R_2:R_3/nm	Separation/nm	Wavelength/nm	E_1	E_2
80:40:20	S_1=4, S_2=2	548	13	14
		408	15	23
		359	6	11
60:30:15	S_1=3, S_2=1.5	479	20	23
		344	4	7
40:20:10	S_1=2, S_2=1	446	32	45
		342	4	5

between the smaller nanowires enhance slightly with the stronger SP coupling at longer wavelength of the resonance peaks. However, for the resonance peak at shorter wavelengths, the electric field enhancement is greatly depressed due to the cancellation of its polarization. Even though the stronger SP coupling and cascade effect exists between the smaller sizes and separations of the homotrimer nanowires, the size effect considerably influences the extinction spectra with lower peak height [30, 31].

To rich and further confirm the calculated results discussed above, the other two sets of homotrimers with radii R_1=225 nm, R_2=75 nm, R_3=25 nm (R_1:R_2:R_3=9:3:1) and R_1=400 nm, R_2=100 nm, R_3=25 nm (R_1:R_2:R_3=16:4:1) are investigated. When the separations are symmetrical and asymmetrical, the resulting ECS spectra, corresponding charge distribution at the multiple resonance peaks and electric field distribution are shown in the supplementary materials (Fig.S5 and S6 and Tables S1 and S2). In addition, the comparable homodimers, which are the fundamental elements of the homotrimer, are also investigated as the reference in Fig.S5 and S6 (supplementary materials). One can note that the bright and dark modes exist in the homodimer and homotrimer. In addition, combined the charge distribution and the electric filed (E_1 and E_2 listed in Tables S1 and S2 of the supplementary materials) between the nanowires, the suppression of the cascade effect is confirmed by the appearance of the bright mode in the homotrimer. In favor of the dark mode, the cascade effect results in the higher electric field distributed between the smaller nanowires. Furthermore, arising from the increasing of the separations, the weakened SP coupling generally results in decreasing electric field.

IV. CONCLUSION

In this work, we have systematically investigated the plasmonic properties of the asymmetrical silver nanowire homotrimer with asymmetrical separation and radius. It is found that, multiple plasmonic properties and different electromagnetic coupling can be generated originated from the coupling between the bright and dark modes, which have been confirmed by the charge distributions at the resonance wavelengths. When the bright mode with radiative damping exists in the homotrimer, the cascade effect is depressed, resulting in the higher electric field distributed in the approaching area of the bigger nanowires. In the opposite way, when the plasmon modes have the dark modes between the smaller nanowires, which can store the electromagnetic energy, the cascade effect results in higher electric field in the gap of the smaller nanowires. The above results are confirmed by three sets of homotrimer with different asymmetrical separations and radii. We believe that the simulated results obtained in this work may be useful for the analysis of the optical behaviors of asymmetrical nanowires while the experimental characterization of the non-uniform samples shows different comparison from the ideally simulation adopted the symmetrical models. In addition, the appearance of the different coupling plasmon modes between the nanowire arrays may be useful to contribute to overcome the light propagation length, which is of importance in waveguides. Nanowire plasmonic waveguides can be generally served as the miniaturization of optical signal processing, data transmission.

Supplementary materials: Table S1, S2 show the electric field at the resonance peaks for the nanowire homotrimer with symmetrical and asymmetrical separations with the parameters of R_1=225 nm, R_2=75 nm, R_3=25 nm (R_1:R_2:R_3=9:3:1) and R_1=400 nm, R_2=100 nm, R_3=25 nm (R_1:R_2:R_3=16:4:1), respectively. Figure S1 shows the charge distribution of the homodimer with the radii R_1=R_2=100 nm at the resonance wavelengths 359, 497, and 826 nm, respectively. Figure S2 shows the influence of the asymmetrically structural parameters of H1 and H2 on the extinction cross section. Figure S3 shows the corresponding charge distribution at the different resonance wavelengths for H1 and H2 with the separation S=4 nm. Figure S4 shows the charge contribution at the resonance peaks 362, 403, 450, and 634 nm, respectively, for the separations S_1=S_2=4 nm as the radii of the homotrimer are R_1=100, R_2=50, and R_3=25 nm. Figure S5 and S6 show the ECS of the nanowire homodimer and homotrimer with asymmetrical separations and radii R_1=225 nm, R_2=75 nm, R_3=25 nm (R_1:R_2:R_3=9:3:1) and R_1=400 nm, R_2=100 nm, R_3=25 nm (R_1:R_2:R_3=16:4:1), respectively, and the corresponding charge distributions at the resonance peaks.

V. ACKNOWLEDGMENTS

This work was supported by the National Basic Research Program of China (No.2012CB932303),

DOI:10.1063/1674-0068/29/cjcp1602030

the National Natural Science Foundation of China (No.51171176, No.51471162, and No.11204307), and the CAS/SAFEA International Partnership Program for Creative Research Teams.

[1] W. L. Barnes, A. Dereux, and T. W. Ebbesen, Nature **424**, 824 (2003) .
[2] J. Aizpurua, P. Hanarp, D. S. Sutherland, M. Kall, G. W. Bryant, and F. J. G. de Abajo, Phys. Rev. Lett. **90**, 057401 (2003).
[3] E. Ozbay, Science **311**, 189 (2006).
[4] K. Li, M. I. Stockman, and D. J. Bergman, Phys. Rev. Lett. **91**, 227402 (2003).
[5] B. Sturman, E. Podivilov, and M. Gorkunov, Europhys. Lett. **101**, 741 (2013).
[6] L. A. Sweatlock, S. A. Maier, and H. A. Atwater, Phys. Rev. B **71**, 235408 (2005).
[7] B. Auguié and W. L. Barnes, Phys. Rev. Lett. **101**, 143902 (2008).
[8] S. Yashna and D. Anuj, Nanotechnology **25**, 210 (2014).
[9] F. Hao, P. Nordlander, Y. Sonnefraud, P. V. Dorpe, and S. A. Maier, ACS Nano. **3**, 643 (2009).
[10] P. K. Jain, S. Eustis, and M. A. El-Sayed, J. Phys. Chem. B **110**, 18243 (2006).
[11] T. G. Habteyes, S. Dhuey, S. Cabrini, P. J. Schuck, and S. R. Leone, Nano Lett. **11**, 1819 (2011).
[12] J. Q. Hu, Q. Chen, Z. X. Xie, G. B. Han, R. H. Wang, B. Ren, Y. Zhang, Z. L. Yang, and Z. Q. Tian, Adv. Funct. Mater. **14**, 183 (2004).
[13] K. D. Wang, H. X. Zhang, and Y. F. Liu, Chin. J. Chem. Phys. **24**, 434 (2011).
[14] Z. L. Netzer, Z. Tanaka, B. Chen, and C. Y. Jiang, J. Phys. Chem. C **117**, 16187 (2013)
[15] G. Liu and J. Shao, Chin. J. Chem. Phys. **24**, 239 (2011)
[16] B. Kenens, M .Rybachuk, J. Hofkens, and H. Uji-I, J. Phys. Chem. C **117**, 2547 (2013).
[17] P. M. Gresho and R. L. Sani, *Absorption and Scattering of Light by Small Particles*, New York: Wiley (2000).
[18] P. B. Johnson and R. W. Christy, Phys. Rev. B **6**, 4370 (1972).
[19] S. Westcott, J. Jackson, C. Radloff, and N. Halas, Phys. Rev. B **66**, 155431 (2002).
[20] F. Hao, E. M. Larsson, T. A. Ali, D. S. Sutherland, and P. Nordlander, Chem. Phys. Lett. **458**, 262 (2008).
[21] O. Pena-Rodríguez, U. Pal, M. Campoy-Quiles, L. Rodríguez-Fernández, M. Garriga, and M. I. Alonso, J. Phys. Chem. C **115**, 6410 (2011).
[22] M. Liu, T. W. Lee, S. K. Gray, P. Guyot-Sionnest, and M. Pelton, Phys. Rev. Lett. **102**, 107401 (2009).
[23] C. J. Xuan, X. D. Wang, L. Xia, B. Wu, H. Li, and S. X. Tian, Chin. J. Chem. Phys. **27**, 628 (2014).
[24] S. Zhang, D. A. Genov, Y. Wang, M. Liu, and X. Zhang, Phys. Rev. Lett. **101**, 047401 (2008).
[25] P. Tassin, L. Zhang, T. Koschny, E. N. Economou, and C. Soukoulis, Phys. Rev. Lett. **102**, 053901 (2009).
[26] A. Manjavacas and F. J. G. Abajo, Opt. Express **17** 19401 (2009).
[27] Y. G. Chen, T. S. Kao, B. Ng, X. Li, X. G. Luo, B. Luk'yanchuk, S. A. Maier, and M. H. Hong, Opt. Express **21**, 13691 (2013).
[28] W. M. Wei, R. H. Z, Y. K. W, F. Yang, and S. Hong, Chin. J. Chem. Phys. **27**, 659 (2014).
[29] W. Cai, L. Wang, X. Zhang, J. Xu, and F. J. G. Abajo, Phys. Rev. B **82**, 125454 (2010).
[30] Z. K. Zhou, X. N. Peng, Z. J. Yang, Z. S. Zhang, M. Li, X. R. Su, Q. Zhang, X. Y. Shan, Q. Q. Wang, and Z. Y. Zhang, Nano Lett. **11**, 49 (2011).
[31] S. Kawata, *Near-Field Optics and Surface Plasmon Polaritons*, Berlin: Springer, (2001).

DOI:10.1063/1674-0068/29/cjcp1602030